ORIGINAL ARTICLE

Microwave-assisted synthesis and antibacterial propensity of N′-s-benzylidene-2-propylquinoline-4-carbohydrazide and N′-((s-1H-pyrrol-2-yl)methylene)-2-propylquinoline-4-carbohydrazide motifs

Olayinka O. Ajani [a,*], King T. Iyaye [a], Damilola V. Aderohunmu [a], Ifedolapo O. Olanrewaju [a], Markus W. Germann [b], Shade J. Olorunshola [c], Babatunde L. Bello [b]

[a] Department of Chemistry, Covenant University, CST, Canaanland, Km 10 Idiroko Road, P.M.B. 1023, Ota, Ogun State, Nigeria
[b] Department of Chemistry, Georgia State University, Atlanta, GA 30302, USA
[c] Department of Biological Sciences, Covenant University, CST, Canaanland, Km 10 Idiroko Road, P.M.B. 1023, Ota, Ogun State, Nigeria

Abstract   Microwave-assisted approach was utilized as green approach to access a series of 2-pro pylquinoline-4-carbohydrazide hydrazone derivatives **10a-j** of aromatic and heteroaromatic aldehydes in highly encouraging yields. It involved four steps reaction which was initiated with ring opening reaction of isatin in a basified environment and subsequent cross-coupling with pentan-2-one to produce compound **7**. Esterification of **7** in acid medium led to the formation of compound **8** which was reacted with hydrazine hydrate to access **9** which upon microwave-assisted condensed with aromatic and heteroaromatic aldehydes furnished the targeted compounds **10a-j**. The structures of **10a-j** were confirmed by physico-chemical, elemental analyses and spectroscopic characterization which include UV, FT-IR, ^{1}H and ^{13}C NMR as well as DEPT-135. The targeted compounds **10a-j**, alongside with gentamicin clinical standard, were investigated for their antibacterial efficacies using agar diffusion method. 2-Propyl-N′-(pyridine-3-ylmethylene) quinoline-4-carbohydrazide **10j** emerged as

* Corresponding author.
E-mail address: ola.ajani@covenantuniversity.edu.ng (O.O. Ajani).
Peer review under responsibility of King Saud University.

ELSEVIER   **Production and hosting by Elsevier**

the best antibacterial hydrazide-hydrazone with lowest MIC value of $0.39 \pm 0.02 - 1.56 \pm 0.02$ µg/mL across all the organisms screened.

1. Introduction

The quinoline nucleus is one of the most prevalent heterocyclic scaffolds and is found in several bio-active natural products (Keri and Patil, 2014; Simoes et al., 2014). Quinoline is a benzo-fused pyridine heterocycle which occurs naturally in Skimmianine which is a furoquinoline alkaloid present mainly in the Rutaceae family (Huang et al., 2017). The 2-phenylquinoline was identified as alkaloid from the plant *Galipea longiflora* (Breviglieri et al., 2017). Quinolines and its derivatives represent a broad class of compounds, which have received considerable attention due to their wide range of pharmacological properties (Khalifa et al., 2017). Owing to high significant of quinoline in medicinal research and other applications, numerous derivatives of this *N*-heterocycle have been synthesized. For the synthesis of quinolines, various methods have been reported including the Pfitzinger (Ibrahim and Al-Faiyz, 2016), Povarov (Almansour et al., 2015), Doebner-Miller (Ishak et al., 2013), Skraup (Pandeya and Tyagi, 2011), Conrad-Limpach (Brouet et al., 2009), Friedlander (Yang et al., 2007), Combes (Parikh et al., 2006). However, the Friedländer condensation is still considered as a popular method for the synthesis of quinoline derivatives (Nasseri et al., 2015) because among all the named reaction for quinoline synthesis, the Friedländer annulation (Ibrahim and Al-Faiyz, 2016) appears to be still one of the most simple and straightforward approaches for the synthesis of quinolines (Marco-Contelles et al., 2009). However, the adopted approach in this present study was Pfitzinger method wherein ring-opening reaction of isatin followed by condensation with aliphatic ketone was engaged (Sonawane and Tripathi, 2013). There are several other established protocols for the synthesis of these ring frameworks (Liao et al., 2017). Synthesis via linking of other molecular entities with quinoline core have been proven to increase bioactivity of the resultant motifs. For instance, synthesis of aliphatic amide bridged 4-aminoquinoline clubbed 1,2,4-triazole derivatives and evaluation of their antibacterial activity against seven different bacterial strains was reported (Thakur et al., 2016). Gold-catalyzed [4 + 2]annulation/cyclization of benzisoxazoles was reported as a viable pathway for accessing highly oxygenated quinoline (Sahani and Liu, 2017).

Furthermore, quinoline moiety is an essential pharmacophore and a crucial functionality because of its wide variety of reported biological and pharmacological activities which include anticancer (Zablotskaya et al., 2017), antibacterial (Sun et al., 2017), anti-inflammatory (Pinz et al., 2017), antioxidant (Murugavel et al., 2017), antitubercular (Bodke et al., 2017), antiproliferative (Nathubhai et al., 2017), antifungal (Ben et al., 2017), antimalarial (Vijayaraghavan and Mahajan, 2017), antiprotozoal (Garcia et al., 2017), antitumor (Fouda, 2017), DNA binding (Krstulović et al., 2017), antihypertensive (Kumar et al., 2015), anti-HIV (Zhong et al., 2015), activities among others. Quinoline based tyrosine kinase inhi-

bitors have proven antidiabetic effect in different animal models and in clinical cancer patients (Orfi et al., 2017). Therapeutic efficacy of quinoline derivatives cannot be overemphasized as they form the core structure of numerous commercially available drugs. Some of the examples are ofloxacin **1**, quinidine **2**, chloroquine **3**, clioquinol **4**, bosutinib hydrate **5** and ivacaftor **6** (Yin et al., 2015) as shown in Fig. 1. Molecular hybrid is one of the most popular strategies to develop new drug candidates based on combination of structural features of two different active fragments, which do not only reduce the risk of drug-drug interactions but also improve the pharmacological activities (Shaveta et al., 2016). In another study, piperazine bridged 4-aminoquinoline 1,3,5-triazine derivatives led to the production of antibacterial agents (Verma et al., 2016).

Antibiotic-resistant bacteria that are difficult or impossible to treat are becoming increasingly common and are causing a global health crisis. For instances, there were reported cases of methicillin-resistance *Staphylococcus aureus* (MRSA) strains (Blair et al., 2015) which are considered to be one of the major causes of food-borne diseases in hospitals (Dehkordi et al., 2017), quinolone-resistant *Escherichia coli* (QREC) which is common in feces from young calves (Duse et al., 2016), multidrug resistant *Proteus vulgaris* (Mandal et al., 2015). In addition, because the importance of fluoroquinolones (FQs) in humans and animals is increasing, FQ-resistant bacteria are a major concern in the treatment of infectious diseases (Hu et al., 2017). The bacteria used in this present study are *S. aureus, Bacillus lichenformis, Proteus vulgaris, Micrococcus varian, Escherichia coli* and *Pseudomonas aeruginosa*. These organisms are great source of potential threat to health and wellbeing of man and his ecosystem because they are causative agents of numerous infectious diseases. Due to drug resistance challenges, emergent of new diseases and high rate of global health threat, there is continuous need for the preparation of biologically active heterocyclic compounds as therapeutic target in drug design. Molecular hybridization approach can address these issues. Hence, we have herein incorporated benzylidene and heteroaromatic methylidene on quinoline moiety through hydrazide linker by microwave assisted technique as green approach in order to evaluate their antimicrobial efficacy via *in vitro* screening for future antimicrobial drug design.

2. Experimental

2.1. Material and methods

All the chemical reagents used herein were purchased from Sigma Aldrich Chemicals except hydrazine hydrate and vanillin which were obtained from Surechem Product Chemicals and Kiran Light Laboratory respectively. They were of analytical grade and were used as received. Stuart melting point apparatus was used to determine the melting points which were uncorrected. The UV–visible analysis was carried out
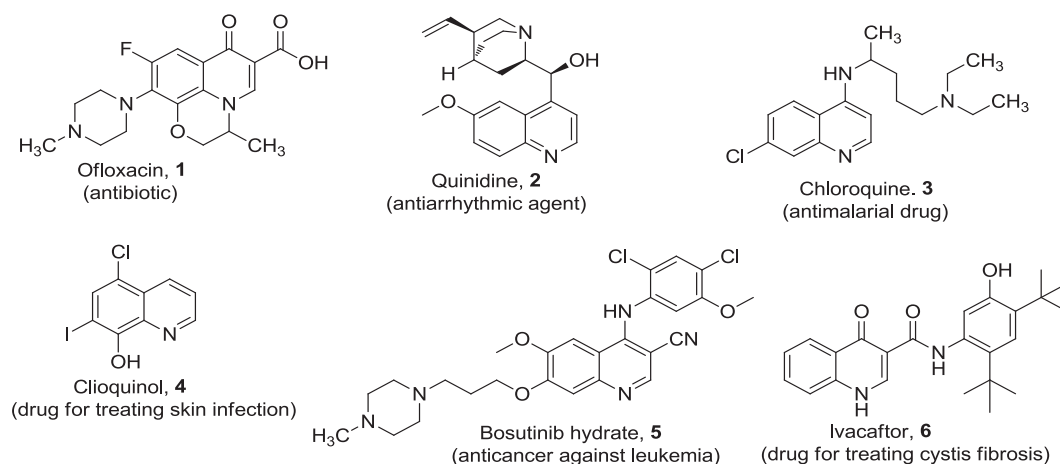
Fig. 1   Some commercially available quinoline-based drugs and their uses.

with the aid of UV-Genesys Spectrophotometer Infrared (IR) spectra were run in KBr pellet using the Perkin Elmer FT-IR Spectrophotometer. The progress of the reaction and the level of purity of the compounds were routinely checked by Thin Layer Chromatography (TLC) on silica gel plates. The ^{1}H NMR and ^{13}C NMR spectra were recorded on NMR Bruker DPX 400 Spectrometer operating at the machine frequencies of 400 MHz and 100 MHz respectively using DMSO-d_6 as solvent. DEPT-135 NMR analysis was evaluated for all the synthesized compounds and Tetramethylsilane (TMS) was used as internal standard. The microwave assisted synthesis were carried out using CEM Discover Monomode oven operating at frequency of 2450 MHz monitored by a PC computer and temperature control was fixed at 140 °C within the power modulation of 500 W. The reactions were performed in sealed tube within ramp time of 1 to 3 min. The elemental analysis (C, H, N) of the synthesized compounds were performed using a Flash EA 1112 elemental analyzer. Selectivity index (S.I.) was calculated by dividing the zones of inhibition of compounds against organisms with the zones of inhibition of gentamicin against organisms.

2.2. Synthetic procedures

2.2.1. General procedure for microwave-assisted synthesis of targeted products (10a-j)

2-Propylquinoline-4-carbohydrazide, **9** (3.0 g, 13 mmol) was dissolved in ethanol (10 mL) in a sealed tube. The corresponding aldehyde (13 mmol) was added and the resulting mixture was then irradiated in microwave oven for a period of 1 to 3 min as the case may be based on the result obtained from the monitored progress of reaction using TLC spotting in dichloromethane (DCM) as eluent. The heated solution was allowed to cool to ambient temperature and filtered to afford the corresponding hydrazide-hydrazone of quinoline (10a-j) in good to excellent yields.

2.2.1.1. N'-Benzylidene-2-propylquinoline-4-carbohydrazide (10a).
Microwave-assisted reaction of **9** (3.0 g, 13 mmol) with benzaldehyde (1.3 mL, 13 mmol) for 1 min afforded N'-benzylidene-2-propylquinoline-4-carbohydrazide, **10a.** Yield 3.84 g, 93%. UV–Vis.: λ_{max} (nm)/log ε_{max} (M^{-1} cm^{-1}): 212 (3.97), 225 (3.99), 236 (4.01), 257 (4.64), 314 (4.21). IR (KBr, cm^{-1}) $\bar{\upsilon}$: 3358 (N—H), 3151 (C—H aromatic), 2943 (C—H aliphatic), 2805 (C—H aliphatic), 1683 (C=O hydrazide), 1604 (C=C aromatic), 1589 (C=N), 1467 (CH$_3$ deformation), 1335 (CH$_2$ deformation), 1248 (C—N of hydrazide), 929 (=C—H bending), 749 (Ar-H). ^{1}H NMR (400 MHz, DMSO-d_6) δ_H: 8.36 (s, 1H), 7.83–7.81 (d, J = 8.40 Hz, 2H, Ar-**H**), 7.75–7.73 (d, J = 8.28 Hz, 2H, Ar-**H**), 7.43–7.40 (m, 3H, Ar-**H**), 7.29–7.26 (dd, J_1 = 8.40 Hz, J_2 = 10.00 Hz 2H, Ar-**H**), 5.80 (s, 1H, N=C—**H**), 3.31–3.25 (q, J = 7.22 Hz, 2H, CH$_2$), 1.97–1.91 (m, 2H, Aliph-**H**), 0.88–084 (t, J = 7.12 Hz, 3H, CH$_3$CH$_2$). ^{13}C NMR (100 MHz, DMSO-d_6) δ_C: 173.3 (C=O), 155.2, 151.0, 146.6, 142.7, 138.1, 134.0 (2 × CH), 132.0, 127.8, 120.8, 117.7, 117.1, 115.2 (2 × CH), 112.6, 110.5, 29.7, 25.2, 15.1 (CH$_3$) ppm. DEPT 135 (100 MHz, DMSO-d_6) δ_C: Positive signals are: 155.2, 138.1, 134.0 (2 × CH), 132.0, 127.8, 117.1, 115.2 (2 × CH), 112.6, 110.5, 15.1 (CH$_3$). Negative signals are: 29.7 (CH$_2$), 25.2 (CH$_2$) ppm.

2.2.1.2. N'-(4-Chlorobenzylidene)-2-propylquinoline-4-carbohydrazide (10b).
Microwave-assisted reaction of **9** (3.0 g, 13 mmol) with 4-chlorobenzaldehyde (1.83 g, 13 mmol) for 1 min afforded N'-(4-chlorobenzylidene)-2-propylquinoline-4-carbohydrazide, **10b.** Yield 4.53 g, 92%. UV–Vis.: λ_{max} (nm)/ log ε_{max} (M^{-1} cm^{-1}): 221 (4.33), 228 (4.25), 250 (4.43), 260 (4.80), 308 (4.78). IR (KBr, cm^{-1}) $\bar{\upsilon}$: 3376 (N—H), 3060 (C—H aromatic), 2943 (C—H aliphatic), 2884 (C—H aliphatic), 1689 (C=O hydrazide), 1616 (C=C aromatic), 1593 (C=N), 1463 (CH$_3$ deformation), 1334 (CH$_2$ deformation), 1202 (C—N of hydrazide), 934 (=C—H bending), 826 (C—Cl), 745 (Ar-H). ^{1}H NMR (400 MHz, DMSO-d_6) δ_H: 8.36 (s, 1H), 7.83–7.81 (d, J = 8.80 Hz, 2H, Ar-**H**), 7.75–7.73 (d, J = 8.20 Hz, 2H, Ar-**H**), 7.29–7.26 (dd, J_1 = 8.20 Hz, J_2 = 10.02 Hz 2H, Ar-**H**), 7.12–7.10 (d, J = 8.80 Hz, 2H, Ar-**H**), 5.80 (s, 1H, N=C—**H**), 3.31–3.25 (q, J = 7.22 Hz, 2H, CH$_2$), 1.96–1.91 (m, 2H, Aliph-**H**), 1.02–0.99 (t, J = 7.12 Hz, 3H, CH$_3$-CH$_2$). ^{13}C NMR (100 MHz, DMSO-d_6) δ_C: 173.2 (C=O), 156.4, 155.2, 142.8 (2 × CH), 138.1, 134.1 (2 × CH), 132.0, 127.5, 117.5, 115.2 (2 × CH), 112.6, 110.5, 29.5, 25.4, 15.3 (CH$_3$) ppm. DEPT 135 (100 MHz, DMSO-d_6) δ_C: Positive signals are: 155.2, 142.8 (2 × CH), 134.1 (2 × CH), 132.0, 127.5, 117.5, 115.2 (2 × CH), 110.5, 15.3 (CH$_3$). Negative signals are: 29.5 (CH$_2$), 25.4 (CH$_2$) ppm.

2.2.1.3. N'-(4-Ethoxybenzylidene)-2-propylquinoline-4-carbo-hydrazide (10c). Microwave-assisted reaction of **9** (3.0 g, 13 mmol) with 4-ethoxybenzaldehyde (1.95 g, 13 mmol) for 3 min afforded N'-(4-ethoxybenzylidene)-2-propylquinoline-4-c arbohydrazide, **10c.** Yield 3.69 g, (73%). UV–Vis.: λ_{max} (nm)/log ε_{max} (M^{-1} cm^{-1}): 225 (4.48), 227 (4.61), 255 (4.62), 272 (5.07), 338 (4.94). IR (KBr, cm^{-1}) $\bar{v}$: 1682 (C=O hydrazide), 1602 (C=C aromatic), 1572 (C=N), 1471 (CH_3 deformation), 1300 (C−N of hydrazide), 1116 (C−O, of OEt), 921 (=C−H bending), 749 (Ar-H). ^{1}H NMR (400 MHz, DMSO-d_6) δ_H: 8.38 (s, 1H), 7.83–7.81 (d, J = 8.60 Hz, 2H, Ar-**H**), 7.74–7.72 (d, J = 8.22 Hz, 2H, Ar-**H**), 7.29–7.26 (dd, J_1 = 8.22 Hz, J_2 = 10.00 Hz 2H, Ar-**H**), 7.12–7.10 (d, J = 8.60 Hz, 2H, Ar-**H**), 5.80 (s, 1H, N=C−**H**), 3.31–3.25 (q, J = 7.16 Hz, 2H, **CH$_2$**CH$_3$), 3.17–3.11 (q, J = 7.22 Hz, 2H, **CH$_2$**), 1.98–1.90 (m, 2H, Aliph-**H**), 1.12–1.08 (t, J = 7.16 Hz, 3H, **CH$_3$**CH$_2$), 1.02–0.99 (t, J = 7.12 Hz, 3H, **CH$_3$**CH$_2$). ^{13}C NMR (100 MHz, DMSO-d_6) δ_C: 173.5 (C=O), 156.2, 155.1, 151.0, 147.3, 142.5 (2 × CH), 135.9, 134.2 (2 × CH), 132.0, 127.5, 117.1, 115.0 (2 × CH), 112.3, 110.7, 47.8, 29.4, 25.0, 20.1, 14.9 (CH$_3$) ppm. DEPT 135 (100 MHz, DMSO-d_6) δ_C: Positive signals are: 142.5 (2 × CH), 134.2 (2 × CH), 132.0, 127.5, 117.1, 115.0 (2 × CH), 110.7, 20.1 (CH$_3$), 14.9 (CH$_3$). Negative signals are: 47.8 (CH$_2$), 29.4 (CH$_2$), 25.0 (CH$_2$) ppm.

2.2.1.4. N'-(3-Methoxybenzylidene)-2-propylquinoline-4-carbo-hydrazide (10d). Microwave-assisted reaction of **9** (3.0 g, 13 mmol) with 3-methoxybenzaldehyde (1.77 g, 13 mmol) for 3 min afforded N'-(3-methoxybenzylidene)-2-propylquinoline-4-carbohydrazide, **10d.** Yield 3.16 g, (65%). UV–Vis.: λ_{max} (nm)/log ε_{max} (M^{-1} cm^{-1}): 215 (4.47), 221 (4.47), 240 (4.58), 257 (4.99), 308 (4.93). IR (KBr, cm^{-1}) $\bar{v}$: 3459 (N−H), 3106 (C−H aromatic), 2923 (C−H aliphatic), 2854 (C−H aliphatic), 1699 (C=O hydrazide), 1622 (C=C aromatic), 1580 (C=N), 1458 (CH$_3$ deformation), 1346 (CH$_2$ deformation), 1245 (C−N of hydrazide), 1185 (C−O, of OMe), 927 (=C−H bending), 719 (Ar-H). ^{1}H NMR (400 MHz, DMSO-d_6) δ_H: 8.38 (s, 1H), 8.13 (s, 1H), 7.83–7.81 (d, J = 8.00 Hz, 1H, Ar-**H**), 7.75–7.73 (d, J = 8.20 Hz, 2H, Ar-**H**), 7.61–7.59 (d, J = 7.80 Hz, 1H, Ar-**H**), 7.42–7.39 (m, 1H, Ar-**H**), 7.29–7.26 (dd, J_1 = 8.20 Hz, J_2 = 10.00 Hz 2H, Ar-**H**), 7.06 (s, 1H, Ar-**H**), 5.80 (s, 1H, N=C−**H**), 3.31–3.25 (q, J = 7.22 Hz, 2H, **CH$_2$**), 2.40 (s, 3H, OCH$_3$), 1.98–1.93 (m, 2H, Aliph-**H**), 1.02–0.99 (t, J = 7.12 Hz, 3H, **CH$_3$**CH$_2$). ^{13}C NMR (100 MHz, DMSO-d_6) δ_C: 173.9 (C=O), 157.4, 154.4, 151.3, 146.6, 141.7, 139.0, 138.1, 134.7 (2 × CH), 132.5, 124.9, 123.3, 120.8, 115.2, 112.3, 110.8, 55.9 (OCH$_3$), 31.9, 24.9, 15.1 (CH$_3$) ppm. DEPT 135 (100 MHz, DMSO-d_6) δ_C: Positive signals are 146.6, 141.7, 138.1, 134.7 (2 × CH), 132.5, 124.9, 120.8, 112.3, 110.8, 55.9 (OCH$_3$), 15.1 (CH$_3$) ppm. Negative signals are: 31.9, 24.9 (CH$_2$) ppm.

2.2.1.5. N'-(2-Nitrobenzylidene)-2-propylquinoline-4-carbohy-drazide (10e). Microwave-assisted reaction of **9** (3.0 g, 13 mmol) with 2-nitrobenzaldehyde (1.96 g, 13 mmol) for 2 min afforded N'-(2-nitrobenzylidene)-2-propylquinoline-4-carbohy drazide, **10e.** Yield 3.86 g, (76%). UV–Vis.: λ_{max} (nm)/log ε_{max} (M^{-1} cm^{-1}): 210 (4.32), 230 (4.41), 237 (4.38), 250 (4.41), 257 (5.11). IR (KBr, cm^{-1}) $\bar{v}$: 3411 (N−H), 3104 (C−H aromatic), 3035 (C−H aromatic), 2913 (C−H aliphatic), 2865 (C−H aliphatic), 1699 (C=O of hydrazide), 1608 (C=C aromatic), 1571 (C=N), 1527 (N−O of NO$_2$), 1447 (CH$_3$ deformation),

1346 (CH$_2$ deformation), 1271 (C−N), 983 (=C−H bending), 743 (Ar-H). ^{1}H NMR (100 MHz, DMSO-d_6) δ_H: 8.36 (s, 1H), 8.16–8.14 (d, J = 7.60 Hz, 1H, Ar-**H**), 7.84–7.82 (d, J = 7.54 Hz, 1H, Ar-**H**), 7.75–7.73 (d, J = 8.20 Hz, 2H, Ar-**H**), 7.29–7.27 (dd, J_1 = 8.20 Hz, J_2 = 10.02 Hz 2H, Ar-**H**), 7.22 (s, 1H, Ar-**H**), 7.12–7.06 (m, 2H, Ar-**H**), 5.80 (s, 1H, N=C−**H**), 3.31–3.25 (q, J = 7.22 Hz, 2H, **CH$_2$**), 1.96–1.91 (m, 2H, Aliph-**H**), 1.02–0.99 (t, J = 7.12 Hz, 3H, **CH$_3$**CH$_2$). ^{13}C NMR (100 MHz, DMSO-d_6) δ_C: 173.2 (C=O), 157.2, 151.2, 146.3, 141.2, 138.5, 138.0, 134.1 (2 × CH), 132.4, 131.6, 126.0, 121.7, 120.3, 117.7, 115.4, 110.3, 31.5, 26.1, 21.0 (CH$_3$) ppm. DEPT 135 (100 MHz, DMSO-d_6) δ_C: Positive signals are 141.2, 138.5, 138.0, 134.1 (2 × CH), 126.0, 120.3, 117.7, 115.4, 110.3, 21.0 (CH$_3$) ppm. Negative signals: 31.5, 26.1 (CH$_2$).

2.2.1.6. N'-(4-Hydroxy-3-methoxybenzylidene)-2-propyl quino-line-4-carbohydrazide (10f). Microwave-assisted reaction of **9** (3.0 g, 13 mmol) with vanillin (1.98 g, 13 mmol) for 2 min afforded N'-(4-hydroxy-3-methoxybenzylidene)-2-propylquino line-4-carbohydrazide, **10f.** Yield 4.73 g (93%). UV–Vis.: λ_{max} (nm)/log ε_{max} ($M^{-1}cm^{-1}$): 221 (4.23), 236 (4.29), 248 (4.31), 278 (4.76), 308 (4.80). IR (KBr, cm^{-1}) $\bar{v}$: 3320 (OH of phenol), 3021 (C−H aromatic), 2977 (C−H aliphatic), 2947 (C−H aliphatic), 2858 (C−H aliphatic), 1681 (C=O of hydrazide), 1620 (C=C), 1575 (C=N), 1464 (CH$_3$ deformation), 1373 (CH$_2$ deformation), 1271 (C−N), 1114 (C−O of OMe), 983 (=C−H bending), 733 (Ar-H). ^{1}H NMR (400 MHz, DMSO-d_6) δ_H: 9.02 (s, 1H, OH), 8.37 (s, 1H), 8.13 (s, 1H), 8.01–7.99 (d, J = 7.60 Hz, 1H, Ar-**H**), 7.76–7.74 (d, J = 8.22 Hz, 2H, Ar-**H**), 7.61–7.59 (d, J = 7.56 Hz, 1H, Ar-**H**), 7.29–7.26 (dd, J_1 = 8.22 Hz, J_2 = 10.00 Hz 2H, Ar-**H**), 7.06 (s, 1H, Ar-**H**), 5.80 (s, 1H, N=C−**H**), 3.31–3.25 (q, J = 7.22 Hz, 2H, **CH$_2$**), 2.40 (s, 3H, OCH$_3$), 1.98–1.93 (m, 2H, Aliph-**H**), 1.02–0.99 (t, J = 7.12 Hz, 3H, **CH$_3$**CH$_2$). ^{13}C NMR (100 MHz, DMSO-d_6) δ_C: 173.0 (C=O), 159.5, 157.4, 154.4, 151.3, 146.6, 141.7, 139.0, 138.1, 134.7 (2 × CH), 132.5, 124.9, 123.3, 120.8, 115.2, 110.8, 55.9 (OCH$_3$), 31.9, 24.9, 15.1 (CH$_3$) ppm. DEPT 135 (100 MHz, DMSO-d_6) δ_C: Positive signals are 146.6, 141.7, 138.1, 134.7 (2 × CH), 132.5, 124.9, 120.8, 115.2, 110.8, 55.9 (OCH$_3$), 15.1 (CH$_3$) ppm. Negative signals: 31.9, 24.9 (CH$_2$) ppm.

2.2.1.7. N'-((1H-pyrrol-2-yl)methylene)-2-propylquinoline-4-carbohydrazide (10g). Microwave-assisted reaction of **9** (3.0 g, 13 mmol) with 1H-pyrrole-2-carbaldehyde (1.24 g, 13 mmol) for 2 min afforded N'-((1H-pyrrol-2-yl)methylene)-2-propylqui noline-4-carbohydrazide, **10g** (88%). Yield 3.50 g (88%). UV–Vis.: λ_{max} (nm)/log ε_{max} (mol^{-1} cm^{-1}): 208 (3.85), 215 (3.90), 224 (3.98), 230 (4.11), 257 (4.46). IR (KBr, cm^{-1}) $\bar{v}$: 3310 (N−H), 3245 (N−H), 3102 (C−H aromatic), 2964 (C−H aliphatic), 2870 (C−H aliphatic), 1681 (C=O of hydrazide), 1621 (C=C), 1588 (C=N), 1452 (CH$_3$ deformation), 1364 (CH$_2$ deformation), 1275 (C−N), 983 (=C−H bending), 744 (Ar-H). ^{1}H NMR (400 MHz, DMSO-d_6) δ_H: 11.05 (s, 1H, N**H**), 8.54 (s, 1H), 8.21 (s, 1H), 7.75–7.73 (d, J = 8.20 Hz, 2H, Ar-**H**), 7.29–7.26 (dd, J_1 = 8.20 Hz, J_2 = 10.08 Hz, 2H, Ar-**H**), 6.95–6.93 (d, J = 7.76 Hz, 1H, Pyrr-**H**), 6.55–6.51 (dd, J_1 = 7.76 Hz, J_2 = 7.94 Hz, 1H, Pyrr-**H**), 6.22–6.20 (d, J = 7.94 Hz, 1H, Pyrr-**H**), 5.80 (s, 1H, N=C−**H**), 3.31–3.25 (q, J = 7.20 Hz, 2H, **CH$_2$**), 1.96–1.91 (m, 2H, Aliph-**H**), 1.02–0.99 (t, J = 7.10 Hz, 3H, **CH$_3$**CH$_2$). ^{13}C NMR (100

MHz, DMSO d_6) δ_C: 173.3 (C=O), 157.6, 155.2, 151.2, 146.8, 143.0, 138.3, 134.3 (2 × CH), 131.4, 125.1, 121.1, 117.1, 112.6, 110.5, 29.9, 25.6, 15.1 (CH$_3$) ppm. DEPT 135 (100 MHz, DMSO-d_6) δ_C: Positive signals are: 155.2, 138.3, 134.3 (2 × CH), 131.4, 125.1, 121.1, 117.1, 110.5, 15.1 (CH$_3$) ppm. Negative signals are: 29.9 (CH$_2$), 25.6 (CH$_2$) ppm.

2.2.1.8. N'-((5-Methyl-1H-pyrrol-2-yl)methylene)-2-propylquinoline-4-carbohydrazide (10h). Microwave-assisted reaction of **9** (3.0 g, 13 mmol) with 5-methyl-1H-pyrrole-2-carbaldehyde (1.42 mL, 13 mmol) for 3 min afforded N'-((5-methyl-1H-pyrrol-2-yl)methylene)-2-propylquinoline-4-carbohydrazide, **10h**. Yield 3.04 g (73%). UV–Vis.: λ_{max} (nm)/log ε_{max} (mol^{-1} cm^{-1}): 203 (4.04), 225 (4.08), 251 (4.10), 254 (4.38), 305 (4.11). IR (KBr, cm^{-1}) $\bar{\upsilon}$: 3443 (N—H), 3362 (N—H), 3059, 3035 (C—H aromatic), 2970 (C—H aliphatic), 2876 (C—H aliphatic), 1687 (C=O of hydrazide), 1614 (C=C), 1575 (C=N), 1461 (CH$_3$ deformation), 1375 (CH$_2$ deformation), 1292 (C—N), 945 (=C—H bending), 725 (Ar-H). ^{1}H NMR (400 MHz, DMSO-d_6) δ_H: 11.04 (s, 1H, **NH**), 8.58 (s, 1H), 8.22 (s, 1H), 7.75–7.73 (d, J = 8.20 Hz, 2H, Ar-**H**), 7.29–7.26 (dd, J_1 = 8.20 Hz, J_2 = 10.08 Hz, 2H, Ar-**H**), 6.83–6.81 (d, J = 7.78 Hz, 1H, Pyrr-**H**), 6.22–6.20 (d, J = 7.78 Hz, 1H, Pyrr-**H**), 5.80 (s, 1H, N=C—**H**), 3.31–3.25 (q, J = 7.22 Hz, 2H, **CH$_2$**), 2.38 (s, 3H, **CH$_3$**), 1.96–1.91 (m, 2H, Aliph-**H**), 1.02–0.99 (t, J = 7.12 Hz, 3H, **CH$_3$**CH$_2$). ^{13}C NMR (100 MHz, DMSO-d_6) δ_C: 173.1 (C=O), 155.1, 151.0, 146.5, 142.8, 138.1, 134.2 (2 × CH), 131.3, 125.1, 121.1, 117.1, 115.0, 112.6, 110.5, 29.9, 25.6, 18.3 (CH$_3$), 15.1 (CH$_3$) ppm. DEPT 135 (100 MHz, DMSO-d_6) δ_C: Positive signals are: 155.2, 138.1, 134.2 (2 × CH), 131.3, 125.1, 117.1, 110.5, 18.3 (CH$_3$), 15.1 (CH$_3$) ppm. Negative signals are: 29.9 (CH$_2$), 25.6 (CH$_2$) ppm.

2.2.1.9. N'-((3,5-dimethyl-1H-pyrrol-2-yl)methylene)-2-propylquinoline-4-carbohydrazide (10i). Microwave-assisted reaction of **9** (3.0 g, 13 mmol) with 3,5-dimethyl-1H-pyrrole-2-carbaldehyde (1.60 mL, 13 mmol) for 3 min afforded N'-((3,5-dimethyl-1H-pyrrol-2-yl)methylene)-2-propylquinoline-4-carbohydrazide, **10i**. Yield 3.51 g (81%). UV–Vis.: λ_{max} (nm)/log ε_{max} (mol^{-1} cm^{-1}): 215 (4.33), 224 (4.43), 240 (4.33), 257 (5.14). IR (KBr, cm^{-1}) $\bar{\upsilon}$: 3374 (N—H), 3303 (N—H), 3036 (C—H aromatic), 2980 (C—H aliphatic), 2889 (C—H aliphatic), 1688 (C=O of hydrazide), 1605 (C=C), 1587 (C=N), 1465 (CH$_3$ deformation), 1355 (CH$_2$ deformation), 1297 (C—N), 983 (=C—H bending), 747 (Ar-H). ^{1}H NMR (400 MHz, DMSO-d_6) δ_H: 11.04 (s, 1H, **NH**), 8.56 (s, 1H), 8.20 (s, 1H), 7.75–7.73 (d, J = 8.20 Hz, 2H, Ar-**H**), 7.29–7.24 (dd, J_1 = 8.20 Hz, J_2 = 11.26 Hz, 2H, Ar-**H**), 6.47 (s, 1H, Pyrr-**H**), 5.80 (s, 1H, N=C—**H**), 3.31–3.25 (q, J = 7.20 Hz, 2H, **CH$_2$**), 2.46 (s, 3H, **CH$_3$**), 2.38 (s, 3H, **CH$_3$**), 1.96–1.91 (m, 2H, Aliph-**H**), 1.02–0.99 (t, J = 7.12 Hz, 3H, **CH$_3$**CH$_2$). ^{13}C NMR (100 MHz, DMSO-d_6) δ_C: 173.3 (C=O), 155.0, 151.0, 146.5, 142.8, 138.1, 134.2 (2 × CH), 131.3, 125.1, 121.1, 116.8, 115.0, 112.6, 110.5, 29.9, 25.6, 18.8 (CH$_3$), 18.3 (CH$_3$), 15.1 (CH$_3$) ppm. DEPT 135 (100 MHz, DMSO-d_6) δ_C: Positive signals are: 155.0, 138.1, 134.2 (2 × CH), 131.3, 125.1, 116.8, 110.5, 18.8 (CH$_3$), 18.3 (CH$_3$), 15.1 (CH$_3$) ppm. Negative signals are: 29.9 (CH$_2$), 25.6 (CH$_2$) ppm.

2.2.1.10. 2-Propyl-N'-(pyridine-3-ylmethylene)quinoline-4-carbohydrazide (10j). Microwave-assisted reaction of **9** (3.0 g, 13

mmol) with 3-pyridine carboxaldehyde (1.22 mL, 13 mmol) for 1ø min afforded 2-propyl-N'-(pyridine-3-ylmethylene)quinoline-4-carbohydrazide, **10j** 4.28 g (96%). UV–Vis.: λ_{max} (nm)/log ε_{max} (M^{-1} cm^{-1}): 221 (4.15), 250 (4.15), 254 (4.47), 314 (4.40), 410 (3.58). IR (KBr, cm^{-1}) $\bar{\upsilon}$: 3419 (N—H), 3059 (C—H aromatic), 2959 (C—H aliphatic), 2865 (C—H aliphatic), 1683 (C=O of hydrazide), 1615 (C=C), 1575 (C=N), 1451 (CH$_3$ deformation), 1367 (CH$_2$ deformation), 1269 (C—N), 1271 (C—N), 934 (=C—H bending), 724 (Ar-H). ^{1}H NMR (400 MHz, DMSO-d_6) δ_H: 8.88 (s, 1H), 8.42 (s, 1H), 8.11 (s, 1H), 7.96–7.94 (d, J = 7.04 Hz, 1H, Pyr-**H**), 7.75–7.73 (d, J = 8.22 Hz, 2H, Ar-**H**), 7.61–7.59 (d, J = 7.46 Hz, 1H, Pyr-**H**), 7.29–7.26 (dd, J_1 = 8.22 Hz, J_2 = 10.08 Hz, 2H, Ar-**H**), 7.08–7.04 (dd, J_1 = 7.04 Hz, J_2 = 7.46 Hz, 1H, Pyr-**H**), 5.80 (s, 1H, N=C—**H**), 3.31–3.25 (q, J = 7.20 Hz, 2H, **CH$_2$**), 1.96–1.90 (m, 2H, Aliph-**H**), 1.02–0.99 (t, J = 7.10 Hz, 3H, **CH$_3$**CH$_2$). ^{13}C NMR (100 MHz, DMSO-d_6) δ_C: 173.5 (C=O), 157.4, 155.1, 151.0, 147.3, 142.8, 138.0, 134.2 (2 × CH), 130.9, 127.3, 121.0, 117.1, 112.5, 110.2, 108.5, 29.9, 25.6, 15.1 (CH$_3$) ppm. DEPT 135 (100 MHz, DMSO-d_6) δ_C: Positive signals are: 155.1, 138.0, 134.2 (2 × CH), 130.9, 127.3, 121.0, 117.1, 110.2, 108.5, 15.1 (CH$_3$) ppm. Negative signals are: 29.9 (CH$_2$), 25.6 (CH$_2$) ppm.

2.3. Antibacterial activity assay

The antibacterial assay of the **10a-j** was investigated against six organisms namely: *Pseudomonas aeruginosa, Staphylococcus aureus, Escherichia coli, Proteus vulgaris, Bacillus lichenformis* and *Micrococcus varians*. The organisms were not type culture; but they were locally isolated organisms which were identified using API Kits and conventional biochemical methods. The clinical standard, gentamicin was used as the positive control and DMSO was used as the solvent for dissolution. Antibacterial sensitivity testing was carried out using agar diffusion method while minimum inhibitory concentration (MIC) test was determined by serial dilution method as described by standard method (Russell and Furr, 1977). To obtain minimum bactericidal concentration (MBC), 0.1 mL volume was taken from each tube and spread on agar plates. The number of c. f.u was counted after 18–24 h of incubation at 35 °C. It was determined from the broth dilution of MIC tests by subculturing to agar plates that do not contain the test agent. The MBC is identified by determining the lowest concentration of antibacterial agent that reduces the viability of the initial bacterial inoculum by a pre-determined reduction such as ≥99.9% (Ajani and Nwinyi, 2010).

3. Results and discussion

3.1. Chemistry

Microwave-assisted reactions have been intensely investigated since the earliest publications (Gedye et al., 1986; Giguerre et al., 1986). Based on the experimental data from various studies that have been reported over three decades ago, chemists have found that, microwave-enhanced chemical reaction rates and can be faster than those of conventional heating methods by as much as a thousand-fold (Hayes, 2004). The emergence of multidrug-resistant bacteria causes an urgent need for new generation of antibiotics, which may have a
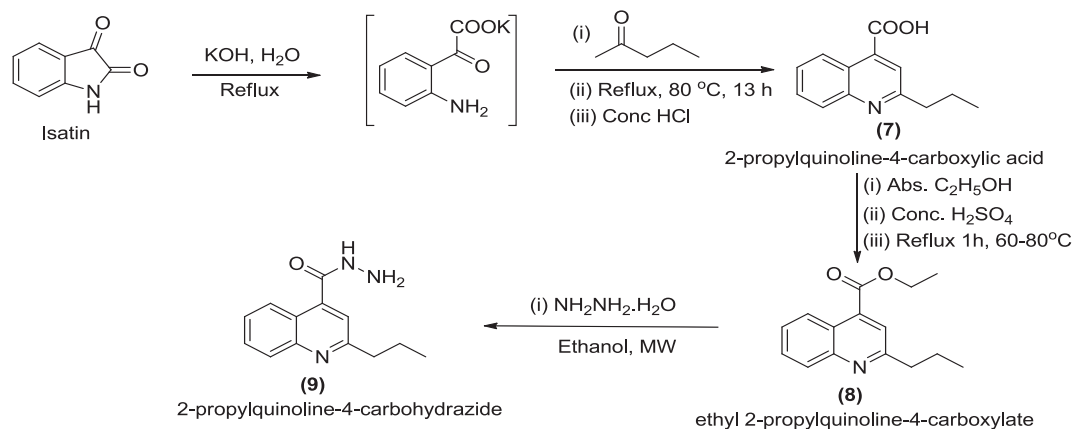
Scheme 1   Pathways for the synthesis of 2-propylquinoline-4-carbohydrazide, **9**.

10a: R = H
10b: R = 4-Cl
10c: R = 4-OEt
10d: R = 3-OMe
10e: R = 2-NO$_2$
10f: R = 3-OMe, 4-OH

(**10a-f**)

10g: R = H
10h: R = 5-Me
10i: R = 3-Me, 5-Me

(**10g-i**)

10j
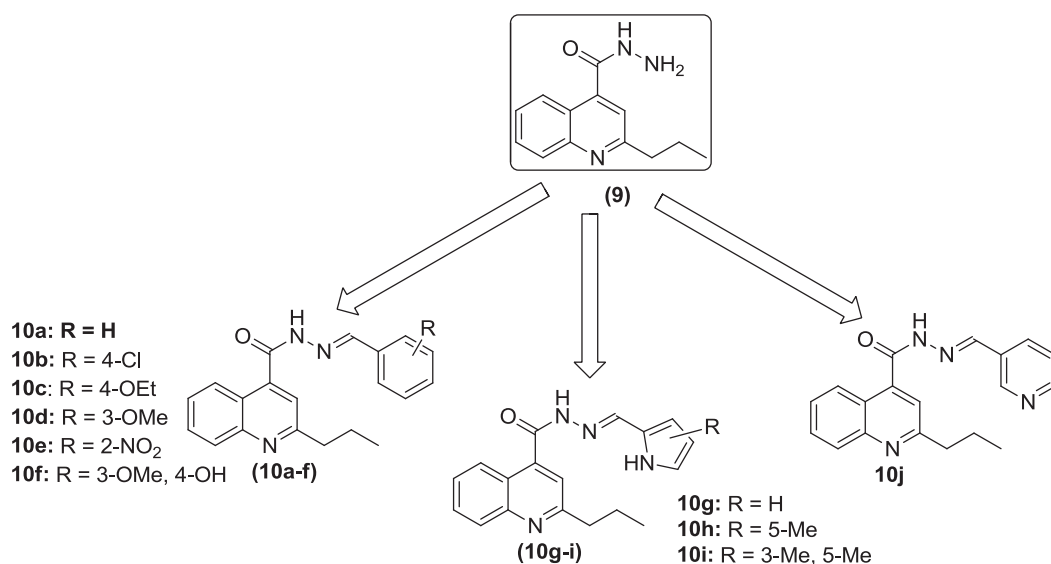
Regents: (a) benzaldehyde **(b)** 4-chlorobenzaldehyde **(c)** 4-ethoxybenzaldehyde **(d)** 3-methoxybenzaldehyde **(e)** 2-nitrobenzaldehyde **(f)** vanillin **(g)** pyrrole-2-carboxaldehyde **(h)** 5-methylpyrrole-2-carboxaldehyde **(i)** 3,5-dimethylpyrrole-2-carboxaldehyde **(j)** nicotinaldehyde. **Reaction Condition:** MW, Ethanol, for 1-3 min, 140 °C

Scheme 2 N'-(Substitutedbenzylidene)-2-propylquinoline-4-carbohydrazide, **10a-j**.

different mechanism of inhibition or killing action from the existing ones (Sun et al., 2017). Thus, in continuation of our research effort on the microwave assisted synthesis of heterocyclic scaffolds (Ajani et al., 2016; Ajani et al., 2010; Ajani and Nwinyi, 2010), we have herein reported the preparation of N'-(s-benzylidene and s-heteroaromatic methylidene)-2-propylquinoline-4-carbohydrazides, **10a-j** in order to investigate their antimicrobial efficacies for possible future drug development. The synthetic pathway adopted to synthesize the reactive intermediate **7–9** and targeted products **10a-j** were as described in Schemes 1 and 2 respectively. The synthesis started with ring-opening reaction of isatin and subsequent cross-coupling with pentan-2-one by heating under reflux for 13 h according to a standard method (Saleh and Khaleel, 2015), to afford 2-propylquinoline-4-carboxylic acid **7** which was esterified to produce ethyl 2-propylquinoline-4-carboxylate **8** which upon hydrazinolysis furnished 2-propylquinoline-4-carbohydrazide **9** in improved yield (Scheme 1).

Microwave assisted reaction of compound **9** with benzaldehyde **an** and its derivatives **b-f** afforded **10a-f** while its reaction with 5-membered heterocycle 1H-pyrrole, **g** and its substituted derivatives **h-i** produced **10g-i** (Scheme 2). Finally, microwave assisted reaction of **9** with 6-membered heterocycle nicotinaldehyde **j** furnished **10j** (Scheme 2). It is interesting to note that the targeted compounds **10a-j** were obtained in good to excellent yields within short reaction times of 1–3 min. in an eco-friendly manner under the influence of microwave irradiation as green approach. According to Table 1, the result of the physicochemical parameters unveiled that the **10i** was produced in highest yield (96%) while **10d** was obtained in lowest yield (65%). The melting points of compounds **10g**, **10h** and **10i** were 271–273 °C, 288–290 °C and 300 °C respectively while all other final products, (**10a-f** and **10j**) refused to melt at 300 °C, except that of **10d** which was not determined because it was oily substance. The visual observation confirmed that colour ranged from brown (**10b, 10g**) to black (**10c, 10d**) to yellow

Table 1 Physico-chemical properties of the synthesized compounds (10a-j).

Comp No	Molecular formula	Mol. Wt.	Yield (%)	Melting pt (°C)	Colour	Elemental analysis (%)Calcd. (Found)		
						C	H	N
10a	$C_{20}H_{19}N_3O$	317.38	93	> 300	Yellow	75.69(75.81)	6.03(5.89)	13.24(13.33)
10b	$C_{20}H_{18}ClN_3O$	351.83	92	> 300	Brown	68.38(68.19)	5.16(4.95)	11.94(12.08)
10c	$C_{22}H_{23}N_3O_2$	361.44	73	> 300	Black	73.11(72.97)	6.41(6.29)	11.63(11.82)
10d	$C_{21}H_{21}N_3O_2$	347.41	65	N.D.	Black	72.60(72.78)	6.09(5.88)	12.10(11.91)
10e	$C_{20}H_{18}N_4O_3$	362.38	76	> 300	Yellow	66.29(66.13)	5.01(4.79)	15.46(15.71)
10f	$C_{21}H_{21}N_3O_3$	363.41	93	> 300	Yellow	69.41(69.62)	5.82(6.01)	11.56(11.78)
10g	$C_{18}H_{18}N_4O$	306.36	88	271–273	Brown	70.57(70.71)	5.92(6.07)	18.29(18.37)
10h	$C_{19}H_{20}N_4O$	320.39	73	288–290	Yellow	71.23(7.09)	6.29(6.11)	17.49(17.26)
10i	$C_{20}H_{22}N_4O$	334.41	81	300 (s)	Orange	71.83(71.74)	6.63(6.45)	16.75(16.89)
10j	$C_{19}H_{18}N_4O$	318.37	96	> 300	Orange	71.68(71.85)	5.70(5.55)	17.60(17.81)

N.D. = Not Determined (oil). Comp. No = Compound Number. (s) = sharp melting point. Mol. Wt. = Molecular weight. Melting Pt = Melting Point.

(10a, 10e, 10f, 10h) to orange (10i-j). The elemental analysis result was consistent with the molecular masses of the compounds and it existed within limit of ± 0.25 between% calculated and% found for C, H, N of the final products 10a-j.

In addition, UV, IR, ^1H and ^{13}C NMR as well as DEPT-135 were used as the spectroscopic means of characterizing the targeted compounds 10a-j. The UV spectra of 10a-j were run in solution using ethanol solvent. The first electronic transition in all the compounds was found at λ_{max} of 203–225 nm. This was as a result of $\pi \to \pi^*$ transition which confirmed the presence of conjugated C=C of benzene which agreed with the value earlier reported for benzene nucleus (Ajani et al., 2016). The longest wavelength λ_{max} of 410 nm found in 10j and other bathochromic shifts experienced were ascribed to the chromophoric C=N group; characteristic of K bands (Komurcu et al., 1995) and existence of some auxochromes which led to $n \to \pi^*$ transitions that originated from the lone pair of electron delocalization ability. FT-IR spectra was run for compounds 10a-j in KBr pellet with vibrational absorption bands appearing at $\bar{\upsilon}$: 3459–3245 cm^{-1}, 3151–3021 cm^{-1}, 2980–2805 cm^{-1}, 1699–1681 cm^{-1}, 1622–1602 cm^{-1}, 1593–1571 cm^{-1}, 1471–1451 cm^{-1}, depicting the presence of N—H, C—H aromatic, C—H aliphatic, C=O hydrazide, C=C aromatic, C=N quinoline/hydrazone, CH$_3$ deformation. Specifically, the presence of a broad band at 3320 cm^{-1} in compound 10f depicted the presence of OH of phenol which was in line with the stretching vibrational frequency of the hydrogen-bonded OH reported by Siyanbola et al. (2017). In addition, the presence of C—N and Ar-H functionalities in all the final products 10a-j was confirmed by the bending vibrational absorption bands at 1300–1202 cm^{-1} and 749–719 cm^{-1} respectively which was in concordance with earlier findings where synthesis and characterization of 2-quinoxalinone-3-hydrazone derivatives was reported (Ajani et al., 2010).

In addition, the chemical shifts and the multiplicity patterns of ^1H- and ^{13}C NMR spectra run in deuterated DMSO were consistent with that of the proposed structures of the title compounds 10a-j. Taking 10a as the representative compound, its ^1H NMR spectrum in a 400 MHz machine showed that 1H of CH of heterocyclic ring resonated downfield at a singlet at δ 8.36 ppm. Also, 2H aromatic doublet signal at δ 7.83–7.81 ppm was due to presence of proton at 5- and 8-positions of quinoline ring, while the remaining 2H on that same benzene

ring at 6- and 7-positions appeared as doublets of doublet at 7.29–7.26 ppm with coupling constant values of 8.40 Hz and 10.00 Hz. The benzylidene 5H of resonated as two signals comprising 2H doublet at δ 7.75–7.73 ppm and 3H multiplet δ 7.43–7.40 ppm. The chemical shift values of the aromatic protons agreed with those earlier reported by Ogunniran et al. (2015) wherein, nicotinic acid hydrazide was utilized as ligand for metal complexes synthesis. The upfield signals outside the aromatic region were recorded between δ 5.80 ppm to δ 0.84 ppm with the most shielded peak being that of 3H triplet of CH$_3$-CH$_2$ at δ 0.88–0.84 ppm having a coupling constant of 7.12 Hz. The ^{13}C NMR spectrum of 10a showed the presence of C=O of hydrazide at 173.3 ppm while the sixteen aromatic carbon atoms and azomethine carbon atoms resonated from 155.2 ppm to 110.5 ppm which were in line with earlier reported ranges for aromatic carbon atoms (Ajani et al., 2016). The aliphatic propyl carbon atom at 2-position appeared as two CH$_2$ at 29.7 ppm and 25.2 ppm while the only CH$_3$ resonated upfield at δ 15.1 ppm. The DEPT 135 showed that there were twelve positive signals which comprised of eleven CH signals and one CH$_3$ signal, while there were two negative signals which depicted the presence of two CH$_2$ signals. These were in accordance with the findings from the ^{13}C NMR result.

3.2. Antibacterial activity

The *in vitro* screening of the synthesized compounds 10a-j and gentamicin standard was carried out on six bacterial isolates (Pseudomonas aeruginosa, Staphylococcus aureus, Escherichia coli, Proteus vulgaris, Bacillus lichenformis and Micrococcus varian) using agar diffusion method (Russell and Furr, 1977). The choice of gentamicin as clinical standard is owing to the fact that it is a bactericidal antibiotic that works by irreversibly binding the 30S subunit of the bacterial ribosome, interrupting protein synthesis (Ajani et al., 2010; Prescott et al., 2005). The result of sensitivity testing of 10a-j with zones of inhibition in mm is as shown in Table 2. It is interesting to note that Pseudomonas aeruginosa was resistant against gentamicin whereas it was sensitive to compounds 10a-j with largest zone of inhibition being 30 mm from 10c and 10j. Although, P. aeruginosa possesses the hardy cell wall which contains porins and efflux pumps called ABC transporters,

Table 2 The result of sensitivity testing of **10a-j** with zones of inhibition in mm.

Compd. No	Organisms used and Z.O.I. (mm)					
	P. aeruginosa	*S. aureus*	*E. coli*	*P. vulgaris*	*B. lichenformis*	*M. varians*
10a	15.00 ± 0.11	16.00 ± 0.13	17.00 ± 0.15	15.00 ± 0.13	13.00 ± 0.11	10.00 ± 0.10
10b	19.00 ± 0.23	19.00 ± 0.17	17.00 ± 0.15	18.00 ± 0.17	15.00 ± 0.14	13.00 ± 0.14
10c	30.00 ± 0.41	23.00 ± 0.25	17.00 ± 0.14	18.00 ± 0.19	13.00 ± 0.12	18.00 ± 0.20
10d	23.00 ± 0.26	17.00 ± 0.15	9.00 ± 0.08	23.00 ± 0.27	11.00 ± 0.12	18.00 ± 0.19
10e	17.00 ± 0.14	30.00 ± 0.39	29.00 ± 0.37	27.00 ± 0.27	25.00 ± 0.22	28.00 ± 0.37
10f	13.00 ± 0.11	33.00 ± 0.42	19.00 ± 0.24	23.00 ± 0.26	18.00 ± 0.19	19.00 ± 0.23
10g	16.00 ± 0.17	17.00 ± 0.15	17.00 ± 0.14	22.00 ± 0.25	25.00 ± 0.21	23.00 ± 0.25
10h	14.00 ± 0.13	15.00 ± 0.14	14.00 ± 0.12	20.00 ± 0.23	22.00 ± 0.20	17.00 ± 0.14
10i	14.00 ± 0.14	16.00 ± 0.16	15.00 ± 0.14	19.00 ± 0.23	21.00 ± 0.21	13.00 ± 0.11
10j	30.00 ± 0.39	34.00 ± 0.41	27.00 ± 0.24	16.00 ± 0.18	29.00 ± 0.38	25.00 ± 0.22
GTM	R	23.00 ± 0.26	25.00 ± 0.21	25.00 ± 0.28	15.00 ± 0.14	18.00 ± 0.20

P. aeruginosa = Pseudomonas aeruginosa, S. aureus = Staphylococcus aureus, E. coli = Escherichia coli, B. lichenformis = Bacillus lichenformis, P. vulgaris = Proteus vulgaris, M. varian = Micrococcus varian. GTM. = Gentamicin, R = Resistance. Mean ± Standard deviation of triplicate measurements. Compd No = Compound No.

which pump out some antibiotics before they are able to act (Prescott et al., 2005), yet synthesized compounds **10a-j** herein inhibited the growth of this organism considerably. Comparing the efficiency of gentamicin with synthesized compounds unveiled that three compounds **10e, 10f** and **10j** inhibited the growth of Staphylococcus aureus at larger Z.O.I. (30–33 mm) than the gentamicin with Z.O.I. of 23 mm. Considering the growth inhibition potential against E. coli, only **10e** (Z.O.I. = 29 mm) and **10j** (Z.O.I. = 27 mm) exhibited larger inhibition zones than gentamicin (Z.O.I. = 25 mm). Low activity experienced in **10d** against E. coli (Z.O.I. = 9 mm) might be due to the protective biofilms formed by this organism. According to the result of the screening against Proteus vulgaris, only **10e** (Z.O.I. = 27 mm) possessed larger inhibitory efficiency than gentamicin (Z.O.I. = 25 mm); although, all the compounds showed considerably improved inhibition with Z.O.I. from 15 mm to 27 mm. Comparative study of activity on Bacillus lichenformis showed that its growth inhibition in **10b** and gentamicin (Z.O.I. = 15 mm) was similar; lower for **10a, 10c, 10d** (Z.O.I. = 11–13 mm) while the rest of the compounds (Z.O.I. = 18–29 mm) exhibited higher inhibitory activity than gentamicin against the growth of Bacillus lichenformis.

Furthermore, both community-associated and hospital-acquired infections with *Staphylococcus aureus* have increased in the past 20 years. In fact, *S. aureus* has been

identified has highly problematic bacterial isolate which has caused high mortality rate in the recent time (Baorto et al., 2017). In view of this, the selectivity index (S.I.) of quinoline hydrazide-hydrazones **10a-j** in comparison with gentamicin, was evaluated against the *S. aureus* (Fig. 2). The comparative study of activity potential of **10a-j** versus that of gentamicin against *S. aureus* was considered since, in humans, gentamicin has structurally different ribosomes from bacteria, thereby allowing the selectivity of this antibiotic for bacteria. Each of the compounds **10b, 10e, 10f,** and **10j** had a better selectivity index (with S.I. > 1) as compared with gentamicin whereas compounds **10a, 10d, 10g, 10h,** and **10i** possessed lesser selectivity indices (S.I. < 1) than gentamicin antibiotic, but **10c** had similar S.I. with gentamicin in the growth inhibition on *S. aureus*. These significant antibacterial activities of the synthesized compounds may be explained with clue of the site of action of hydrazones and hydrazides, where it interacts with bases of DNA of the organisms, and thus, inserts (intercalates) between the stacked bases of helix. This insertion possibly causes a stretching of the DNA duplex and the DNA polymerase is fooled into inserting an extra base opposite an intercalated molecule thereby results to frame shifts. The frame shifts invariably will affect the physiological activity by not arraying the right bases that confer resistance on the organisms (Ajani et al., 2010).
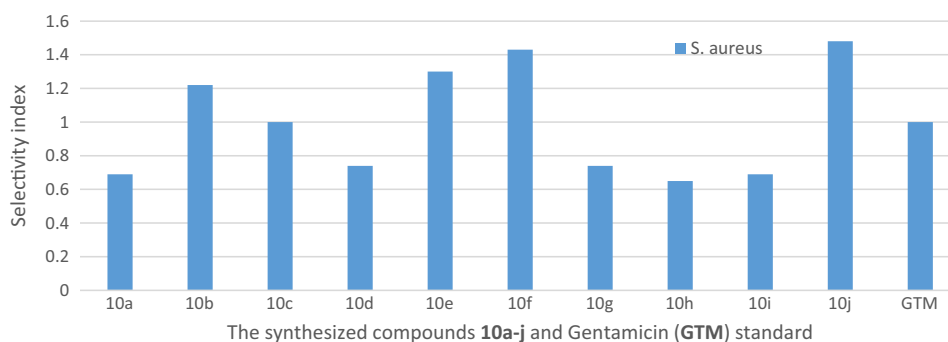
Fig. 2   Result of the selectivity index of hydrazide-hydrazones **(10a-j)** against *S. aureus*.

Table 3 The result of minimum inhibitory concentration (MIC) in µg/mL.

| Sample	Organism used (µg/mL)					
	P. aeruginosa	*S. aureus*	*E. coli*	*B. lichenformis*	*P. vulgaris*	*M. varians*
10a	25.00 ± 0.11	6.25 ± 0.10	12.50 ± 0.05	6.25 ± 0.08	3.13 ± 0.03	6.25 ± 0.09
10b	12.50 ± 0.10	0.78 ± 0.02	0.39 ± 0.02	12.50 ± 0.09	3.13 ± 0.02	3.13 ± 0.03
10c	1.56 ± 0.02	0.39 ± 0.04	1.56 ± 0.02	0.78 ± 0.02	1.56 ± 0.02	3.13 ± 0.02
10d	3.13 ± 0.02	0.39 ± 0.02	25.00 ± 0.12	1.56 ± 0.02	6.25 ± 0.08	3.13 ± 0.02
10e	1.56 ± 0.02	0.39 ± 0.03	0.78 ± 0.03	0.78 ± 0.02	0.78 ± 0.02	0.78 ± 0.03
10f	1.56 ± 0.02	0.39 ± 0.02	3.13 ± 0.03	1.56 ± 0.03	6.25 ± 0.04	0.78 ± 0.02
10g	3.13 ± 0.03	6.25 ± 0.03	0.39 ± 0.02	0.78 ± 0.03	0.78 ± 0.03	3.13 ± 0.02
10h	6.25 ± 0.03	6.25 ± 0.04	12.50 ± 0.04	3.13 ± 0.03	1.56 ± 0.03	1.56 ± 0.02
10i	12.50 ± 0.08	6.25 ± 0.03	12.50 ± 0.08	1.56 ± 0.02	3.13 ± 0.03	3.13 ± 0.03
10j	1.56 ± 0.02	0.39 ± 0.02	0.78 ± 0.02	1.56 ± 0.02	0.39 ± 0.02	0.78 ± 0.02

P. aeruginosa = Pseudomonas aeruginosa, S. aureus = Staphylococcus aureus, E. coli = Escherichia coli, B. licheniformis = Bacillus lichen-formis, P. vulgaris = Proteus vulgaris, M. varian = Micrococcus varian. Mean ± Standard deviation of triplicate measurements.

The minimum inhibitory concentration (MIC) of the synthesized compounds **10a-j** against the six screened organisms was achieved by a standard procedure (Russell and Furr, 1977) and the result is as shown in Table 3. Generally speaking, the MIC values of the compounds **10a-j** ranged from 0.39 ± 0.02 µg/mL to 25.00 ± 0.12 µg/mL. However, critical studies among the benzylidenes **10a-f** showed that non-substituted benzylidene **10a** (R = H) had lowest potency ($3.13 \pm 0.03 – 25.00 \pm 0.11$ µg/mL) while the substituted benzylidenes **10b-f** exhibited improved activity with **10c** (R = 4-OCH$_2$CH$_3$) being the most potent ($0.39 \pm 0.02 – 1.56 \pm 0.02$ µg/mL). This implied that presence of ethoxy substituent, an electron donating group, at para position of benzylidene conferred the highest potency as far as benzylidene groups **10a-f** were concerned. On the contrary, five membered non-substituted heteroaromatic methylidene-containing compound, **10g** ($0.39 \pm 0.02 – 12.50 \pm 0.03$ µg/mL) showed a better efficiency than the substituted counterparts **10h-i** ($1.56 \pm 0.02 – 12.50 \pm 0.08$ µg/mL) while six membered non-substituted heteroaromatic methylidene-containing compound **10j** ($0.39 \pm 0.02 – 1.56 \pm 0.02$ µg/mL) had highest potency among **10a-j** against all the six organisms. From the result of the MIC test, therefore, order of activity of the three most significant compounds against the six organisms was **10j > 10c**

> 10g. Since, all the compounds are structurally related at the quinoline nucleus, it is obvious that nitrogen heteroatom of pyridine in **10j** and of pyrrole in **10g** played significant role in the antibacterial diversity of the compounds. On the overall, compound **10j** emerged as the most active antibacterial agent because it has the lowest MIC value against all the six organisms. Having obtained highly impressed MIC values in the *in vitro* antibacterial screening, the Minimum Bactericidal Concentration (MBC) testing was conducted using standard method as earlier reported (Ajani and Nwinyi, 2010). MBC is the lowest concentration at which 99.9% of the inoculum was killed. The MBC of all the compounds against all the organisms were twofold higher than their MIC except in the activity of compound **10a** against *Pseudomonas aeruginosa* wherein the MBC was found to be the same fold concentration with the MIC (Fig. 3).

3.3. Structure activity relationship (SAR) study

The establishment of the SAR model is essential in order to obtain a deeper insight into the molecular description of compounds' activities. Since all the derivatives as structurally related at their quinoline-hydrazides congeners' end; hence,
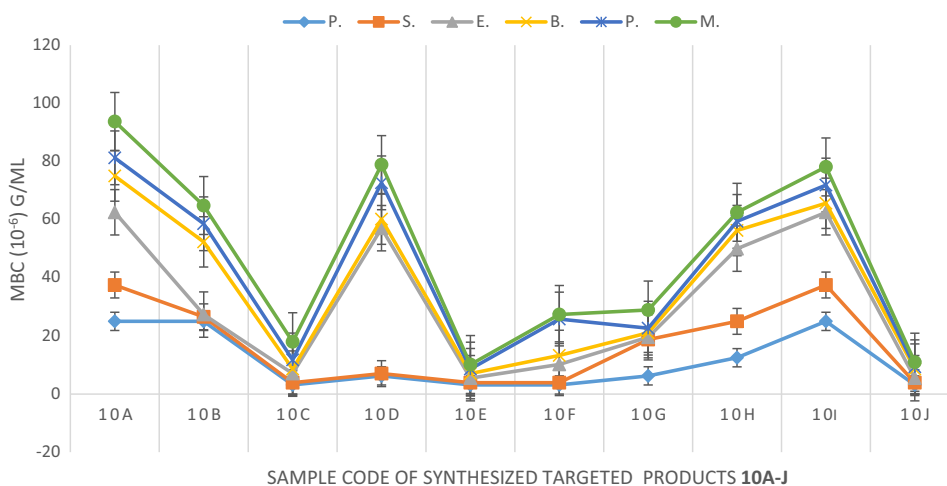
Fig. 3 Graphical representation of minimum bactericidal concentration (MBC).

the variation in antibacterial activities could be traced to either the nature / position of substituents in phenyl-linked hydrazone for **10a-f** and on the numbers of membered-ring nature in the *N*-heterocyclic-linked hydrazones **10g-j**. Therefore, the substitutions on aryl ring of these analogues were varied so as to understand this phenomenon. Comparing the substitution patterns of the phenyl linked hydrazones, **10a-f**, on the growth inhibition against *P. aeruginosa,* the non-substituted phenyl, **10a** (R = H) was the least active (MIC = 25 µg/mL; MBC = 25 µg/mL). The most active compounds among this series of **10a-f** were compounds **10c** (4-OEt), **10e** (2-NO$_2$) and **10f** (4-OH), against the growth of *S. aeruginosa* (MIC = 1.56 µg/mL; MBC 3.13 µg/mL). This was a strong indication that the presence of electron donating group (EDG) at position 4 and electron withdrawing group (EWG) at position 2 had crucial effects on the activity increase observed on the growth inhibition experienced on *S. aeruginosa* as far as phenyl ring substitution was concerned. On the contrary, when electron withdrawing substituent (EWG) was on position 4 (Cl) as seen in **10b**, there was activity decrease (MIC = 12.50 µg/mL; MBC 25.00 µg/mL). This showed that a careful selection of EWG and EDG and their point of attachment on phenyl ring is a worthwhile adventure in the activity scale of preference for phenyl-linked hydrazones **10a-f**. The SAR study of the pyrrole-linked hydrazones series **10g-i** and pyridine-linked hydrazone **10j** against *S. aeruginosa* unveiled the order of antibacterial activity to be **10j > 10g > 10h > 10i**. This implied **10j** (MIC = 1.56 µg/mL; MBC 3.13 µg/mL) which was a non-substituted six-membered heterocycle here conferred more activity on the quinoline-based templates than any of the five-membered heterocyclic pyrrole derivatives **10g-i**. Furthermore, non-substituted pyrrole **10g** (MIC = 3.13 µg/mL; MBC 6.25 µg/mL) was twofold more active than monosubstituted one, **10h** (MIC = 6.25 µg/mL; MBC 12.50 µg/mL) which was in turn twofold more active than disubstituted pyrrole-linked **10i** (MIC = 12.50 µg/mL; MBC 25.00 µg/mL). It means that the presence or increase in numbers of EDGs on pyrrolo or heterocyclic-linked hydrazones led to loss of activity.

4. Conclusions

In conclusion, microwave-assisted synthesis of title compounds **10a-j** was successfully achieved in good to excellent yields. Structural elucidation of the compounds was correctly established since the spectral data information conformed vividly to the proposed structures of **10a-j**. All compounds exhibited broad spectrum of antimicrobial activity against six bacterial isolates with large zones of inhibition in mm. Compound **10j** emerged as the best antimicrobial hydrazide hydrazone with the lowest MIC value of 0.39 ± 0.02 – 1.56 ± 0.02 µg/mL. This compound possesses envisaged candidature for further pharmacological study for future antimicrobial drug development.

Acknowledgments

Conflict of interest

The authors have declared that there is no conflict of interest.

Appendix A. Supplementary material

Supplementary data associated with this article can be found, in the online version, at https://doi.org/10.1016/j.arabjc.2018.01.015.

References

Ajani, O.O., Obafemi, C.A., Nwinyi, O.C., Akinpelu, D.A., 2010. Microwave assisted synthesis and antimicrobial activity of 2-quinoxalinone-3-hydrazone derivatives. Bioorg. Med. Chem. 18 (1), 214–221.

Ajani, O.O., Ajayi, O., Adekoya, J.A., Owoeye, T.F., Durodola, B.M., Ogunleye, O.M., 2016. Comparative study of microwave-assisted and conventional synthesis of 3-[1-(*s*-phenyl imino) ethyl]-2*H*-chromen-2-ones and selected hydrazone derivatives. J. Appl. Sci. 16 (3), 77–87.

Ajani, O.O., Nwinyi, O.C., 2010. Microwave assisted synthesis and evaluation of antimicrobial activity of 3-{3-(*s*-aryl and *s*-heteroaromatic)acryloyl}-2*H*-chromen-2-one derivatives. J. Heterocycl. Chem. 47, 179–187.

Almansour, A., Arumugam, N., Kumar, R.S., Menendez, C., Ghabbour, H., Fun, H.-K., Kumar, R.R., 2015. Straightfoward synthesis of pyrrolo[3, 4-*b*]quinolines through intramolecular Povarov reactions. Tetrahedron Lett. 56, 6900–6903.

Baorto, E.P., Baorto, D., Windle, M.L., Lutwick, L.I., Steele, R.W. 2017. Staphylococcus aureus infection clinical presentation. Medscape Medical News. <http://emedicine.medscape.com/ article/971358-clinical> (accessed 12 August 2017).

Ben, Y.D., Shadkchan, Y., Albert, N., Kontoyiannis, D.P., Osherov, N., 2017. The quinoline bromoquinol exhibits broad-spectrum antifungal activity and induces oxidative stress and apoptosis in *Aspergillus fumigatus*. J. Antimicrob. Chemother. 72 (8), 2263–2272.

Blair, J.M.A., Webber, M.A., Baylay, A.J., Ogbolu, D.O., Piddock, L. J.V., 2015. Molecular mechanisms of antibiotic resistance. Nat. Rev. Microbiol. 13, 42–51.

Bodke, Y.D., Shankerrao, S., Kenchappa, R., Telkar, S., 2017. Synthesis, antibacterial and antitub ercular activity of novel Schiff bases of 2-(1-benzofuran-2-yl)quinoline-4-carboxylic acid derivatives. Russ. J. Gen. Chem. 87, 1843–1849.

Breviglieri, E., da Silva, L.M., Boeing, T., Somensi, L.B., Cury, B.J., Gimenez, A., Filho, V.C., de Andrade, S.F., 2017. Gastroprotective and anti-secretory mechanism of 2-phenyl quinoline, an alkaloid isolated from *Galipea longiflora*. Phytomedicine 25, 61–70.

Brouet, J.C., Gu, S., Peet, N.P., Williams, J.A.D., 2009. A survey of solvents for the Conrad-Limpach synthesis of 4-hydroxyquinolones. Synth. Commun. 39 (9), 5193–5196.

Dehkordi, F.S., Gandomi, H., Basti, A.A., Misaghi, A., Rahimi, E., 2017. Phenotypic and genotypic characterization of antibiotic resistance of methicillin-resistant *Staphylococcus aureus* isolated from hospital food. Antimicrob. Resist. Infect. Control. 6, 104. https://doi.org/10.1186/s13756-017-0257-1.

Duse, A., Waller, K.P., Emmanuelson, U., Unnerstad, H.E., Persson, Y., Bengtsson, B., 2016. Occurrence and spread of quinolone-resistant Escherichia coli on dairy farms. Appl. Environ., Microbiol. 82 (13), 3765–3773.

Fouda, A.M., 2017. Halogenated 2-amino-4pyrano[3,2-*h*]quinoline-3-carbonitriles as antitumor agents and structure-activity relationships of the 4-, 6- and 9-positions. Med. Chem. Res. 26, 302–313.

Garcia, E., Coa, J.C., Otero, E., Carda, M., Vélez, I.D., Robledo, S. M., Cardona, W.I., 2017. Synthesis and antiprotozoal activity of furanchalcone-quinoline, furanchalcone-chromone and furanchalcone-imidazole hybrids. Med. Chem. Res. https://doi.org/10.1007/s00044-017-2076-6.

Gedye, R., Smith, F., Westaway, K., Ali, H., Baldisera, L., Laberge, L., Roussel, J., 1986. The use of microwave ovens for rapid organic synthesis. Tetrahedron Lett. 27 (3), 279–282.

Giguerre, R.J., Bray, T.L., Duncan, S.M., Majetich, G., 1986. Application of commercial micro-wave oven to organic synthesis. Tetrahedron Lett. 27 (41), 4945–4948.

Hayes, B.L., 2004. Recent advances in microwave-assisted synthesis. Aldrichim. Acta 37 (2), 66–76.

Hu, Y.S., Shin, S., Park, Y.H., Park, K.T., 2017. Prevalence and mechanism of fluoroquinolone resistance in Escherichia coli isolated from swine feces in Korea. J. Food Protect. 80 (7), 1145–1151.

Huang, A., Xu, H., Zhan, R., Chen, W., Liu, J., Chi, Y., Chen, D., Ji, X., Luo, C., 2017. Metabolic profile of Skimmianine in rats determined by ultra-performance liquid chromatography coupled with quadrupole time-of-flight tandem mass spectrometry. Molecules 22, 489. https://doi.org/10.3390/molecules22040489 12 pp.

Ibrahim, E., Al-Faiyz, Y., 2016. A simple one-pot synthesis of quinoline-4-carboxylic acids by the Pfitzinger reaction of isatin with enaminones in water. Tetrahedron Lett. 57, 110–112.

Ishak, C., Wahbi, H., Mohamed, M., 2013. Synthesis and characterization of some new 6-substituted-2, 4-di (hetar-2-yl)quinolines via micheal addition-ring closure reaction of schiff base N-(hetar-2-yl) methylene aniline with hetarylketones. Int. J. Pharm. Phytopharmacol. Res. 2 (6), 431–435.

Keri, R.S., Patil, S.A., 2014. Quinoline: A promising antitubercular target. Biomed. Pharmacother. 68, 1161–1175.

Khalifa, N.M., Al-Omar, M.A., El-Galil, A.A.A., El-Reheem, M.A., 2017. Anti-inflammatory and analgesic activities of some novel carboxamides derived from 2-phenyl quinoline candidates. Biomed. Res. 28 (2), 869–874.

Komurcu, S.G., Rollas, S., Uglen, M., Gorrod, J.W., 1995. Evaluation of some arylhydrazones of p-amino benzoic acid hydrazide as antimicrobial agents and their in-vitro hepatic microsomal metabolism. Boll. Chim. Farmac. 134, 375–379.

Krstulović, L., Stolić, I., Jukić, M., Opačak-Bernardi, T., Starčević, K., Bajić, M., Glavaš-Obrovac, L., 2017. New quinoline-arylamidine hybrids: Synthesis, DNA/RNA binding and tumor activity. Eur. J. Med. Chem. 137, 196–210.

Kumar, H., Devaraji, V., Joshi, R., Jadhao, M., Ahirkar, P., Prasath, R., Bhavana, P., Gosh, S.K., 2015. Antihypertensive activity of a quinoline appended chalcone derivative and its site-specific binding interaction with a relevant target carrier protein. RSC Adv. 5, 65496–65513.

Liao, G., Song, H., Yin, X.S., Shi, B.F., 2017. Expeditious synthesis of pyrano[2,3,4-de] quino lines via Rh-catalyzed cascade C-H activation/annulation/lactonization of quinoline-4-ol with alkynes. Chem. Commun. 53, 7824–7827.

Mandal, D., Dash, S.K., Das, B., Sengupta, M., Kundu, P.K., Roy, S., 2015. Isolation and characterization of multi-drug resistance Proteus vulgaris from clinical samples of UTI infected patients from Midnapore, West Bengal. Int. J. Life Sci. Pharm. Res. 5 (2), 32–45.

Marco-Contelles, J., Pérez-Mayoral, E., Samadi, A., do Carmo Carreiras, M., Soriano, E., 2009. Recent advances in Friedländer reaction. Chem. Rev. 109 (6), 2652–2671.

Murugavel, S., Stephen, C.S.J.P., Subashini, R., AnanthaKrishnan, D., 2017. Synthesis, structural elucidation, antioxidant, CT-DNA binding and molecular docking studies of novel chloroquinoline derivatives: Promising antioxidant and anti-diabetic agents. J. Photochem. Photobiol. 173, 216–230.

Nasseri, M.A., Zakerinasab, B., Kamayestani, S., 2015. Proficient procedure for preparation of quinoline derivatives catalyzed by NbCl5 in glycerol as green solvent. J. Appl. Chem., 7 https://doi.org/10.1155/2015/743094.

Nathubhai, A., Haikarainen, T., Koivunen, J., Murthy, S., Koumanov, F., Lioyd, M.D., Holman, G.D., Pihlajaniemi, T., Tosh, D., Lehtiö, L., Threadgill, M.D., 2017. Highly potent and isoform selective dual site binding Tankyrase/Wnt signaling inhibitors that increase cellular glucose uptake and have antiproliferative activity. J. Med. Chem. 60 (2), 814–820.

Ogunniran, K.O., Mesubi, M.A., Raju, K.V.S.N., Narender, T., 2015. Structural and in vitro anti-tubercular activity study of (E)-N'- (2,6-dihydroxybenzylidene)nicotinohydrazide and some transition metal complexes. J. Iran. Chem. Soc. 12, 815–829.

Orfi, Z., Waczek, F., Baska, F., Szabadkai, I., Torka, R., Hartmann, J., Orfi, L., Ullrich, A., 2017. Novel members of quinoline compound family enhance insulin secretion in RIN-5AH beta cells and in rat pancreatic islet microtissue. Sci. Rep. 7, 44073. https://doi.org/10.1038/srep44073.

Pandeya, S.N., Tyagi, A., 2011. Synthetic approaches for quinoline and isoquinoline. Int. J. Pharm. Pharm. Sci. 3 (3), 53–61.

Parikh, A., Parikh, H., Parikh, K., 2006. Name Reactions in Organic Synthesis. Foundation Books, UK, Cambridge.

Pinz, M.P., Reis, A.S., de Oliveira, R.L., Voss, G.T., Vogt, A.G., do Sacramento, M., Roehrs, J.A., Alves, D., Luchese, C., Wilhelm, E. A., 2017. 7-Chloro-4-phenylsulfonyl quinoline, a new antinociceptive and anti-inflammatory molecule: Structural improvement of a quinoline derivate with pharmacological activity. Regul. Toxicol. Pharmacol. 90, 72–77.

Prescott, L.M., Harley, J.P., Donald, K.A., 2005. In Microbiology. McGraw Hill.

Russell, A.D., Furr, J.R., 1977. Antibacterial activity of a new chloroxylenol preparation containing ethylenediamine tetraacetic acid. J. Appl. Bacteriol. UK 43, 253–260.

Sahani, R.L., Liu, R.S., 2017. Gold-catalyzed [4 + 2] annulation/cyclization cascades of benzisoxa zoles with propiolate derivatives to access highly oxygenated tetrahydroquinolines. Angew. Chem. Int. Ed. 56, 12736–12740.

Saleh, M.M., Khaleel, M.I., 2015. Synthesis of isatine derivatives considering Pfitzinger reaction part 1. Int. J. Sci. Res. 4 (8), 2083–2089.

Shaveta, Mishra, S., Singh, P., 2016. Hybrid molecules: The privileged scaffolds for various pharmaceuticals. Eur. J. Med. Chem. 124, 500–536.

Simoes, J.B., de Fatima, A., Sabino, A.A., Almeida Barbosa, L.C., Fernandes, S.A., 2014. Efficient synthesis of 2,4-disubstitued quinolines: Calix[n]arene-catalyzed Povarov-hydrogen-transfer reaction cascades. RSC Adv. 4, 18612–18615.

Siyanbola, T.O., Akinsola, A.F., Obanla, O.R., Adebisi, A.A., Akinsiku, A.A., Olanrewaju, I.O., Ogunniran, K.O., Taiwo, O.S., Ajanaku, K.O., Bamgboye, O.A., 2017. Studies on the antibacterial and anticorrosive properties of synthesized hybrid polyurethane composites from castor seed oil. Rasayan J. Chem. 10 (3), 1003–1014.

Sonawane, R., Tripathi, R., 2013. The chemistry and synthesis of 1H-indole-2,3-dione (isatin) and its derivatives. Int. Lett. Chem. Phys. Astron. 7 (1), 30–36.

Sun, N., Du, R.L., Zheng, Y.Y., Huang, B.H., Guo, Q., Zhang, R.F., Wong, K.Y., Lu, Y.J., 2017. Antibacterial activity of N-methyl-benzofuro[3,2-b]quinoline and N-methylbenzoindolo [3,2-b]-quinoline derivatives and study of their mode of action. Eur. J. Med. Chem. 135, 1–11.

Thakur, A., Gupta, P.R.S., Pathak, P., Kumar, A., 2016. Design, synthesis, SAR, docking and antibacterial evaluation: Aliphatic amide bridged 4-aminoquinoline clubbed 1,2,4-triazole derivatives. Int. J. ChemTech. Res. 9 (3), 629–634.

Verma, A., Prateek, P., Thakur, A., Shukla, P.J., 2016. Piperazine bridged 4-aminoquinoline 1,3,5-triazine derivatives: Design, synthesis, characterization and antibacterial evaluation. Int. J. ChemTech. Res. 9, 261–269.

Vijayaraghavan, S., Mahajan, S., 2017. Docking, synthesis and antimalarial activity of novel 4-anilinoquinoline derivatives. Bioorg. Med. Chem. Lett. 27 (8), 1693–1697.

Yang, D., Jiang, K., Li, J., Xu, F., 2007. Synthesis and characterization of quinoline derivatives via the Friedländer reaction. Tetrahedron 63, 7654–7658.

Yin, D., Wang, W., Peng, Y., Ge, Z., Cheng, T., Wang, X., Li, R., 2015. Synthesis of furo[3,4c] quinolin-3(1H)-one derivatives through TMG catalyzed intramolecular aza-MBH reaction based on the furanones. RSC Adv. 5 (22), 17296–17299.

Zablotskaya, A., Segal, I., Geronikaki, A., Shestakova, I., Nikolajeva, V., Makarenkova, G., 2017. N-Heterocyclic choline analogues based on 1,2,3,4-tetrahydro(iso)quinoline scaffold with anticancer and anti-infective dual action. Pharmacol. Rep. 69, 575–581.

Zhong, F., Geng, G., Chen, B., Pan, T., Li, Q., Zhang, H., Bai, C., 2015. Identification of benzene sulfonamide quinoline derivatives as potent HIV-1 replication inhibitors targeting Rev protein. Org. Biomol. Chem. 13, 1792–1799.